

Compensation of Coarse Quantization Effects on Channel Estimation and BER in Massive MIMO

Reza Mohammadkhani, Azad Azizzadeh, Seyed Vahab Al-Din Makki, John Thompson, and Maziar Nekovee

Abstract—Low-resolution quantization is essential to reduce implementation cost and power consumption in massive multiple-input multiple-output (MIMO) systems for 5G and 6G. While most existing studies assume perfect channel state information (CSI), we model the impact of coarse quantization noise on both channel estimation and data transmission, yielding a more realistic assessment of system performance under imperfect CSI conditions in the uplink. We develop a tight approximation for the bit-error ratio (BER) of uncoded M-QAM with zero-forcing detection, based on the linear minimum mean-square error (LMMSE) channel estimate. These analytical results enable compensation strategies that jointly optimize quantization resolution, transmit power, and pilot length across different numbers of users and base station antennas. We further demonstrate the applicability of the proposed framework through several design scenarios that highlight its effectiveness in optimizing system parameters and improving energy efficiency under quantization constraints. For example, in a 16-QAM system, extending the pilot sequence by 2.5 times and lowering transmit power by 0.5 dB enables a 3-bit quantized system to match the BER of the full-resolution case. The proposed framework offers a fast and accurate alternative to Monte Carlo simulations, enabling practical system optimization under realistic quantization constraints.

Index Terms—Bit error ratio (BER), low resolution ADC, coarse quantization, massive MIMO, 5G, 6G.

I. INTRODUCTION

A. Motivation and Background

MASSIVE MIMO, as a cornerstone of 5G and a foundational element in 6G research, enables base stations (BSs), equipped with hundreds of antennas, to serve multiple users simultaneously, regardless of whether those users have single or multiple antennas [1]. However, having a large number of antennas and radio frequency (RF) chains in massive MIMO results in increased cost, energy consumption, and hardware complexity. A common solution is to use low-resolution analog-to-digital converters (ADCs), which consume significantly less power and have simpler designs that reduce hardware cost and complexity [2]–[6]. They also produce less data, which eases the load on interconnects and digital processing, and makes massive MIMO systems

more scalable and efficient. Nevertheless, using low-resolution ADCs, particularly 1-bit, can degrade system performance due to increased quantization noise. This raises a key question: *Can we maintain performance while benefiting from low-resolution quantization?*

Achieving a balance between reduced quantization resolution and acceptable performance loss remains one of the main challenges in using low-resolution ADCs.

B. Related Works

Numerous studies have explored the performance limitations introduced by low-resolution quantization from various perspectives, considering different performance metrics and system scenarios. Several studies have investigated the capacity of massive MIMO systems with low-resolution quantizers in the uplink mode for maximum ratio combining (MRC), zero-forcing (ZF), and minimum mean-square error (MMSE) detectors [7]–[9]. These works, using the additive quantization noise model (AQNM) and assuming perfect channel state information (CSI), have provided approximations of the achievable rate under Rayleigh fading channels.

The impact of reduced quantization resolution on channel estimation has been the focus of several studies. In [10], the authors considered systems with 1-bit ADCs, employing a least-squares (LS) channel estimator and analyzing the achievable rate using maximum ratio combining (MRC) detectors. In a similar context, [11] used an MMSE estimator to optimize the pilot length for improving the spectral efficiency. Based on Bussgang’s theorem, [12] and [13] reformulated the linear MMSE (LMMSE) estimator for 1-bit and multi-bit resolutions, respectively, and derived achievable rates for MRC and ZF detectors. Additional research has focused on Rician channels with imperfect CSI, using the AQNM model to assess achievable rates for ZF [14] and MRC [15] detection schemes.

In [16], the uplink achievable rate of wideband massive MIMO systems using orthogonal frequency-division multiplexing (OFDM) with 1-bit ADCs was investigated, taking channel estimation errors into account. To reduce power consumption and enhance achievable rates, mixed-architectures (combining low- and high-resolution ADCs) have been proposed in [17] and [18]. These works present approximations of the achievable rate for such architectures in the uplink, using the AQNM model for Rician channels and Bussgang’s model for Rayleigh channels, respectively.

Additionally, for massive MIMO systems with full-duplex and relay configurations, [5], [19]–[23] evaluated achievable

Corresponding author: R. Mohammadkhani.

R. Mohammadkhani and M. Nekovee are with the School of Engineering and Informatics, University of Sussex, UK. (e-mail: mohammadkhani@sussex.ac.uk, m.nekovee@sussex.ac.uk).

A. Azizzadeh is with the Electrical and Computer Engineering Department, IAU, Saqez Branch, Iran (e-mail: azad.azizzadeh@iau.ac.ir)

S. V. Makki is with the Electrical Engineering Department, Razi University, Kermanshah, Iran (e-mail: v.makki@razi.ac.ir).

J. Thompson is with the School of Engineering, University of Edinburgh, UK (email: john.thompson@ed.ac.uk).

rates and energy efficiency under low-resolution quantisation, primarily using the AQNM model. However, none of the aforementioned studies have considered the type and order of modulation in their analytical frameworks. Although the study [12] included modulation effects, it ultimately relied on Monte Carlo simulations to complete its analysis. Studies [6], [24] have also explored the ergodic capacity while accounting for modulation, although they still relied on the assumption of perfect CSI.

Most existing studies have focused on analyzing system capacity, while bit error ratio (BER) analysis and the impact of modulation type have received less attention. However, BER is a fundamental metric for assessing the reliability and quality of service (QoS) in practical communication systems. Furthermore, in massive MIMO systems and the 3GPP standard, high-order modulation schemes such as 16-QAM, 64-QAM, and 256-QAM are used [25]. Coarse quantization introduces significant distortion in such high-order modulation formats. As a result, analyzing the BER in such scenarios becomes increasingly important and serves as a complement to capacity-focused studies.

Although some studies have addressed error performance metrics, many have focused on analyzing the Symbol Error Ratio (SER) under perfect CSI conditions [26]–[30]. However, SER is less applicable in practical systems than BER, as it lacks bit-level resolution. The number of studies that specifically investigate BER remains limited, and a substantial portion are based solely on simulation results [31]–[33].

Existing analytical studies are also confined to specific cases; for example, BER has been analyzed only for QPSK modulation in the downlink mode under perfect CSI [34], [35], or without considering the effect of quantization noise during channel estimation [36]. A study in [37] examines the BER performance of M-QAM modulation schemes in a uniform circular array-based orbital angular momentum (UCA-OAM) transmission model under perfect CSI, using the AQNM model. It performs an analytical assessment up to a certain point and completes the remaining analysis through simulations.

In our previous work, we proposed an analytic upper bound for the BER performance, which was derived under the assumption of perfect CSI [38]. However, in practical scenarios, quantization noise not only degrades user data but also introduces errors in channel estimation, further reducing system performance compared to the perfect CSI case.

C. Contributions

In this study, we extend our previous work in [38] by incorporating quantization noise effects in both the channel estimation and data transmission phases. Then, we assess the BER performance of low-resolution massive MIMO systems under imperfect CSI, providing a more realistic evaluation of coarse quantization effects. Based on accurately derived expressions, we further analyze the influence of system parameters, examine trade-offs, and propose mitigation strategies.

The proposed analytical expressions enable *fast and accurate prediction of system performance*, serving as an efficient

alternative to time-consuming and computationally intensive Monte Carlo simulations. They facilitate optimal parameter selection to achieve a target BER, particularly in scenarios where certain parameters are constrained. In addition, they can be integrated into adaptive architectures [39], [40], combined with machine learning or AI algorithms for improved decision making [41], [42], or even used to generate training data for such models.

While some existing studies offer valuable channel estimation expressions for different quantized systems [12], [13], [18], [19], [21], these results are not directly applicable to our system model. To ensure analytical consistency and accurately capture the effects of quantization noise under the AQNM framework, we derive an LMMSE estimator specifically adapted to our assumptions. This derivation is essential for incorporating channel estimation error into our performance analysis and forms the foundation of our subsequent contributions.

- We develop an analytical framework that captures the effects of coarse quantization on both channel estimation and data transmission under imperfect CSI. Within this framework, we obtain closed-form expressions for the LMMSE channel estimate and the signal-to-interference-plus-quantization-and-noise ratio (SIQNR), and derive a tight BER approximation for uncoded M-QAM with zero-forcing detection.
- We show that the derived expressions enable joint optimization of key system parameters, such as pilot length, transmit power, and quantization resolution, to mitigate quantization-induced performance degradation and achieve BER levels comparable to full-precision systems. Moreover, we provide an exact formula in (24), that specifies how these parameters should be adjusted to achieve full-precision performance.
- We systematically analyze and validate several practical design scenarios, including balancing parameters to match unquantized BER levels, compensating for performance loss as user count increases, selecting power-efficient quantization resolutions, determining the minimum number of antennas for a target user load and BER, and scaling users under quality-of-service constraints.

D. Paper Outline

The remainder of this paper is structured as follows. Section II describes the system model and a linear quantization model to investigate the effects of coarse quantization on both the channel estimation and the data detection stages. In Section III, we derive an LMMSE channel estimate in the presence of quantization error and analyze how it is affected by different parameters (quantization resolution, transmit power, and pilot length). Next, we present an SIQNR and a BER expression in Section IV, taking into account the channel estimation error and quantization error. Monte Carlo simulations are performed in Section V to validate our proposed analytical expressions. Finally, Section VI concludes the paper.

Notations: Bold lowercase and uppercase letters denote vectors and matrices, respectively. The superscripts $(\cdot)^T$ and

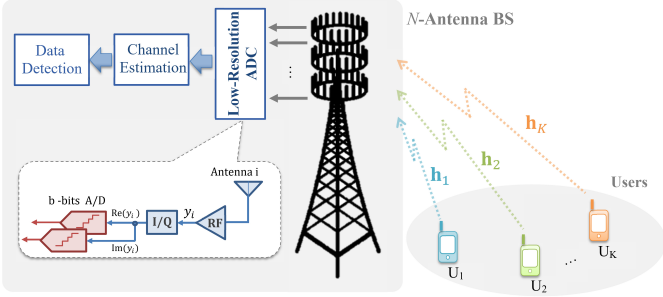


Fig. 1: An uplink quantized massive MIMO system with K single-antenna users and one BS having N antennas.

$(\cdot)^H$ represent the transpose and the Hermitian (conjugate transpose). \mathbb{C} denotes the set of complex numbers, and $\mathbb{E}\{\cdot\}$ stands for expectation. \mathbf{I}_N is the $N \times N$ identity matrix, $\text{diag}(\cdot)$ forms a diagonal matrix from its argument, $\text{Tr}(\cdot)$ denotes the trace, and $\|\cdot\|_F$ represents the Frobenius norm.

II. SYSTEM MODEL

We consider a single cell uplink massive MIMO system with K single-antenna users transmitting their signals to the BS equipped with N -antennas. This is illustrated in Fig. 1. We assume the users transmit a symbol vector $\mathbf{s} \in \mathbb{C}^{K \times 1}$ where each symbol s_k has a constellation size M and $E\{|s_k|^2\} = 1$. Assuming a flat-fading (single-carrier in OFDM) channel model, the received symbol vector $\mathbf{y} \in \mathbb{C}^{N \times 1}$ at the BS, can be written as

$$\mathbf{y} = \sqrt{p_u} \mathbf{H} \mathbf{s} + \mathbf{n} = \sqrt{p_u} \sum_{k=1}^K \mathbf{h}_k s_k + \mathbf{n} \quad (1)$$

where $\mathbf{H} \triangleq [\mathbf{h}_1, \mathbf{h}_2, \dots, \mathbf{h}_K] \in \mathbb{C}^{N \times K}$ denotes the channel matrix, and $\mathbf{h}_k \in \mathbb{C}^{N \times 1}$ is the channel vector between the k th user and the BS. The transmit vector of the users is denoted by $\mathbf{s} = [s_1, s_2, \dots, s_K]^T$, and $\mathbf{n} \in \mathbb{C}^{N \times 1}$ is the additive white Gaussian noise vector. The entries of \mathbf{n} are assumed to be i.i.d Gaussian random variables with zero-mean, unit variance, and are statistically independent of \mathbf{H} . The average transmit power of all users is assumed to be equal and is denoted by p_u , which also represents the average signal-to-noise ratio (SNR) for each user.

We see from Fig. 1 that $2N$ identical b -bit resolution quantizers are needed for the real and imaginary parts of the complex received signals for all antennas. The resulting quantized signal vector can be written as

$$\mathbf{y}_q = Q(\mathbf{y}) = Q(\text{Re}(\mathbf{y})) + jQ(\text{Im}(\mathbf{y})) \quad (2)$$

where $Q(\cdot)$ is the quantization function. The nonlinear nature of quantization process complicates the analysis of low-resolution systems. To enable a more tractable analysis, the AQNM model is employed in this work, offering sufficient accuracy in low and moderate SNR regimes and facilitating the analysis of quantized systems [43], [44]. This model provides valuable insights into the performance of such systems and has been widely used in various types of quantized MIMO systems [7]–[9], [14], [15], [5], [21]–[23], [37], [2]–[4].

TABLE I: values of α and ρ for b -bit resolution ADCs

| b | 1 | 2 | 3 | 4 | 5 |
|----------|--------|--------|---------|----------|----------|
| α | 0.6366 | 0.8825 | 0.96546 | 0.990503 | 0.997501 |

Assuming identical b -bit resolution ADCs for all received signals, we have [7]

$$\mathbf{y}_q = Q(\mathbf{y}) \approx \alpha \mathbf{y} + \mathbf{n}_q \quad (3)$$

where α is the linear gain, and \mathbf{n}_q is the Gaussian quantization noise vector, uncorrelated with the input vector \mathbf{y} . Having non-uniform and low resolution quantizers with bit-resolution of $b \leq 5$, the values of α are shown in Table I. For higher bit-resolution of $b > 5$, an approximate of $\alpha = 1 - \frac{\pi\sqrt{3}}{2}2^{-2b}$ can be applied. For a fixed channel realization \mathbf{H} , the covariance matrix of \mathbf{n}_q can be written as [7]

$$\begin{aligned} \mathbf{R}_{\mathbf{n}_q \mathbf{n}_q} &= \mathbb{E}\{\mathbf{n}_q \mathbf{n}_q^H | \mathbf{H}\} \approx \alpha(1 - \alpha) \text{diag}(\mathbf{R}_{\mathbf{y}\mathbf{y}}) \\ &= \alpha(1 - \alpha) \text{diag}(p_u \mathbf{H} \mathbf{H}^H + \mathbf{I}_N) \end{aligned} \quad (4)$$

III. CHANNEL ESTIMATION FOR COARSELY QUANTIZED MASSIVE MIMO SYSTEMS

In massive MIMO, the BS estimates the channel matrix \mathbf{H} from uplink pilot signals to enable signal detection and downlink precoding. Assuming a Rayleigh block-fading channel (constant over T symbols), the transmission consists of τ pilot symbols followed by $(T - \tau)$ data symbols. We consider equal transmit power for pilots and data, a practical case when users cannot adjust power between these transmission phases [45].

Let $\mathbf{S}_p \in \mathbb{C}^{K \times \tau}$ be the pilot matrix for all users where $\mathbf{s}_{pi} \in \mathbb{C}^{1 \times \tau}$ is the pilot vector of i th user, and $\mathbb{E}\{|s_p(i, j)|^2\} = 1$. Considering equal pilot length of τ (number of pilot symbols) for all users and orthogonality between each pair of pilot vectors, we can write $\mathbf{S}_p \mathbf{S}_p^H = \tau \mathbf{I}_K$. Thus, the received signal of BS at the stage of channel estimation is given by

$$\mathbf{Y}_p = \sqrt{p_u} \mathbf{H} \mathbf{S}_p + \mathbf{N}_p \quad (5)$$

where $\mathbf{Y}_p \in \mathbb{C}^{N \times \tau}$ is the received signal matrix, and $\mathbf{N}_p \in \mathbb{C}^{N \times \tau}$ is the additive white Gaussian noise matrix. The entries of \mathbf{N}_p are assumed to be independent and identically distributed (i.i.d) Gaussian random variables with zero-mean and unit-variance, and are also independent of the channel matrix \mathbf{H} .

The LMMSE estimator of the channel matrix \mathbf{H} from the observation matrix \mathbf{Y}_p can be expressed as $\hat{\mathbf{H}} = \mathbf{Y}_p \mathbf{W}$, where $\mathbf{W} \in \mathbb{C}^{\tau \times K}$ denotes the matrix of complex weights chosen to solve the following minimization problem

$$\hat{\mathbf{H}} = \arg \min_{\hat{\mathbf{H}}} \mathbb{E}\{\|\mathbf{H} - \hat{\mathbf{H}}\|_F^2\} = \arg \min_{\mathbf{W}} \mathbb{E}\{\|\mathbf{H} - \mathbf{Y}_p \mathbf{W}\|_F^2\} \quad (6)$$

For the scenario of full quantization resolution, substituting (5) into (6) and solving yields the channel estimate based on the LMMSE estimator as below [46]:

$$\hat{\mathbf{H}} = \sqrt{p_u} \mathbf{Y}_p \mathbf{S}_p^H (p_u \mathbf{S}_p \mathbf{S}_p^H + \mathbf{I}_K)^{-1} \quad (7)$$

The channel estimation error is defined as $\mathbf{e} = \mathbf{H} - \hat{\mathbf{H}}$. Assuming a Rayleigh distributed channel (\mathbf{H}) with zero-mean and unit-variance entries, the estimate $\hat{\mathbf{H}}$ and the error \mathbf{e} are orthogonal, with both having i.i.d. zero-mean complex Gaussian entries. It can be shown that [47]

$$\sigma_{\hat{h}}^2 = \frac{\tau p_u}{1 + \tau p_u}, \quad \sigma_e^2 = \frac{1}{1 + \tau p_u} \quad (8)$$

where $\sigma_{\hat{h}}^2$ and σ_e^2 are the variances of $\hat{h}_{i,k}$ and $e_{i,k}$, respectively, for $i = 1, \dots, N$ and $k = 1, \dots, K$.

In full-precision quantization, the channel is estimated from the non-quantized $N \times \tau$ complex matrix \mathbf{Y}_p , with the LMMSE estimator considering only the additive white Gaussian noise (AWGN). However, practical massive MIMO employing low-resolution quantizers, require the use of the quantized signal \mathbf{Y}_{pq} . Using the AQNM linear quantizer model,

$$\begin{aligned} \mathbf{Y}_{pq} &= Q(\mathbf{Y}_p) \approx \alpha \mathbf{Y}_p + \mathbf{N}_{qp} = \alpha \sqrt{p_u} \mathbf{H} \mathbf{S}_p + [\alpha \mathbf{N}_p + \mathbf{N}_{qp}] \\ &= \alpha \sqrt{p_u} \mathbf{H} \mathbf{S}_p + \mathbf{N}_e \end{aligned} \quad (9)$$

where \mathbf{N}_{qp} is the quantization noise matrix. Note that \mathbf{N}_{qp} is not a quantized version of \mathbf{N}_p in (5). We define \mathbf{N}_e as the combined quantization and additive noise. One might suggest replacing \mathbf{Y}_p in (7) with \mathbf{Y}_{pq} to obtain the quantized channel estimate. However, this approach only considers AWGN and ignores quantization noise. Thus, we need to substitute \mathbf{Y}_{pq} in the optimization problem (6) and solve it again.

Lemma 1. *The LMMSE estimate of the channel \mathbf{H} from the quantized received signal vector \mathbf{Y}_{pq} in (9), is given by*

$$\hat{\mathbf{H}}_q = \frac{1}{\alpha} \sqrt{p_u} \mathbf{Y}_{pq} \mathbf{S}_p^H (p_u \mathbf{S}_p \mathbf{S}_p^H + L(\alpha, p_u) \mathbf{I}_K)^{-1} \quad (10)$$

where

$$L(\alpha, p_u) = 1 + \left(\frac{1-\alpha}{\alpha}\right)(K p_u + 1) \quad (11)$$

Proof: The proof is given in Appendix A. ■

Lemma 2. *Given the orthogonality between the LMMSE channel estimate $\hat{\mathbf{H}}_q$ in (10) and its estimation error $\mathbf{e}_q = \mathbf{H} - \hat{\mathbf{H}}_q$, and assuming that both $\hat{\mathbf{H}}_q$ and \mathbf{e}_q have i.i.d. zero-mean complex Gaussian entries, it follows that*

$$\sigma_{\hat{h}_q}^2 = \frac{\tau p_u}{L(\alpha, p_u) + \tau p_u}, \quad \sigma_{e_q}^2 = \frac{L(\alpha, p_u)}{L(\alpha, p_u) + \tau p_u} \quad (12)$$

Proof: These results are proved in Appendix B. ■

Building on (12), we can examine the impact of varying the low-resolution quantization on channel estimation as follows.

A. Increasing the quantization resolution

Returning to Table I, as we increase the bit-resolution of the quantizers (ADCs at the uplink receiver in our model), the value of α approaches 1. As a result, $L(\alpha, p_u)$ which is a positive real number, decreases toward 1. Consequently, the variances $\sigma_{\hat{h}_q}^2$ and $\sigma_{e_q}^2$ in (12) approach their corresponding values of $\sigma_{\hat{h}}^2$ and σ_e^2 in (8).

B. Increasing the transmit power

When the transmit power p_u increases toward infinity, in the absence of quantization error as in (8), the estimation error variance σ_e^2 goes to zero. In contrast, with low-resolution quantization as shown in (12), we find that:

$$\sigma_{e_q}^2 \xrightarrow{p_u \rightarrow \infty} \frac{(1-\alpha)K}{(1-\alpha)K + \alpha\tau} \quad (13)$$

This asymptotic behavior indicates that in the presence of quantization error, increasing transmit power alone cannot eliminate the total channel estimation error. However, this error can be reduced by either increasing the bit-resolution of quantizers ($\alpha \rightarrow 1$) or by extending the pilot length τ , or by optimizing both parameters concurrently.

C. Effects of pilot length

Examining (8) and (12) reveals that an increase in the pilot sequence length τ leads to a decrease in both $\sigma_{e_q}^2$ and σ_e^2 , corresponding to the channel estimation error for quantized and non-quantized pilots, respectively. However, this improvement is more significant for the non-quantized case, due to the fact that σ_e^2 in (8) is only a function of τ and the transmit power p_u , while $\sigma_{e_q}^2$ in (12) is affected by more parameters.

One may ask: *What pilot length τ_q is required for a low-resolution quantized system to achieve the same estimation error as the non-quantized scenario with pilot length τ ?*

Starting with a desired target $\sigma_{e_q}^2(\tau_q) \leq \sigma_e^2(\tau)$, we have

$$\tau_q \geq \tau \left(\frac{p_u}{p_{uq}}\right) L(\alpha, p_{uq}) \quad (14)$$

where p_u and p_{uq} are the transmit power for full-precision and low-resolution quantized scenarios, respectively. The function $L(\cdot, \cdot)$ is defined in (11). This expression reveals that it is possible to compensate the performance loss due to low-resolution quantization by jointly optimizing τ_q and p_{uq} , when K , α , τ , and p_u are known.

We further analyze this finding in the following sections, focusing on the BER performance of quantized massive MIMO systems.

IV. SIQNR AND BER OF QUANTIZED MASSIVE MIMO WITH IMPERFECT CSI

Using linear detectors, the K symbol streams for the K users are extracted from the received symbol vector \mathbf{y} at the BS by applying a detection matrix $\mathbf{A} \in \mathbb{C}^{K \times N}$ as $\hat{\mathbf{s}} = \mathbf{A}^H \mathbf{y}$, where \mathbf{A} for zero-forcing (ZF) detection is given by $\mathbf{A} = \mathbf{H}(\mathbf{H}^H \mathbf{H})^{-1}$ [8].

Following [38], we now consider a low-resolution quantized system, in which the quantized received vector \mathbf{y}_q from (3) is used instead of \mathbf{y} to update the detection matrix. Furthermore, in practice, the BS does not have perfect channel state information and an estimate $\hat{\mathbf{H}}$ or $\hat{\mathbf{H}}_q$ is substituted for \mathbf{H} to update the detection matrix. Thus, we can rewrite the detection matrix \mathbf{A} for a coarsely quantized system as

$$\mathbf{A} = \frac{1}{\alpha} \hat{\mathbf{H}}_q (\hat{\mathbf{H}}_q^H \hat{\mathbf{H}}_q)^{-1} \quad (15)$$

In order to obtain the BER of such system, we need to calculate the SIQNR of data streams for each user from the detector output $\hat{\mathbf{s}}$. By employing (15), we obtain

$$\begin{aligned}\hat{\mathbf{s}} &= \mathbf{A}^H \mathbf{y}_q \approx \mathbf{A}^H (\alpha \mathbf{y} + \mathbf{n}_q) \\ &= \frac{1}{\alpha} (\hat{\mathbf{H}}_q^H \hat{\mathbf{H}}_q)^{-1} \hat{\mathbf{H}}_q^H (\alpha \sqrt{p_u} \mathbf{H} \mathbf{s} + \alpha \mathbf{n} + \mathbf{n}_q) \\ &= \frac{1}{\alpha} (\hat{\mathbf{H}}_q^H \hat{\mathbf{H}}_q)^{-1} \hat{\mathbf{H}}_q^H (\alpha \sqrt{p_u} (\hat{\mathbf{H}}_q + \mathbf{e}_q) \mathbf{s} + \alpha \mathbf{n} + \mathbf{n}_q) \\ &= \sqrt{p_u} \mathbf{s} + \left[(\hat{\mathbf{H}}_q^H \hat{\mathbf{H}}_q)^{-1} \hat{\mathbf{H}}_q^H (\sqrt{p_u} \mathbf{e}_q \mathbf{s} + \mathbf{n} + \frac{1}{\alpha} \mathbf{n}_q) \right] \\ &= \sqrt{p_u} \mathbf{s} + \mathbf{n}_e\end{aligned}\quad (16)$$

We refer to \mathbf{n}_e as the *effective noise*, which accounts for the additive white Gaussian noise \mathbf{n} , quantization noise \mathbf{n}_q , and channel estimation error $\mathbf{e}_q = \mathbf{H} - \hat{\mathbf{H}}_q$. To find the SIQNR of each user, we need to calculate the covariance matrix of \mathbf{n}_e as shown in (17).

Assuming equal transmission power for all users, we can write the SIQNR of the k th user as

$$\gamma_{q,k} = \frac{p_u}{[K p_u \sigma_{e_q}^2 + L(\alpha, p_u)]} \frac{1}{[(\hat{\mathbf{H}}_q^H \hat{\mathbf{H}}_q)^{-1}]_{kk}} \quad (18)$$

The channel estimate $\hat{\mathbf{H}}_q$ can be normalized as $\bar{\mathbf{H}} = \hat{\mathbf{H}}_q / \sigma_{\hat{h}_q}$, where entries in $\bar{\mathbf{H}}$ are i.i.d Rayleigh distributed random variables with zero-mean and unit-variances. Substituting this normalized channel into (18) gives

$$\begin{aligned}\gamma_{q,k} &= \frac{p_u \sigma_{\hat{h}_q}^2}{[K p_u \sigma_{e_q}^2 + L(\alpha, p_u)]} \frac{1}{[(\bar{\mathbf{H}}^H \bar{\mathbf{H}})^{-1}]_{kk}} \\ &= \gamma_0 \frac{1}{[(\bar{\mathbf{H}}^H \bar{\mathbf{H}})^{-1}]_{kk}}\end{aligned}\quad (19)$$

where $\sigma_{\hat{h}_q}^2$ and $\sigma_{e_q}^2$ are given in (12). Since $\bar{\mathbf{H}}$ is Rayleigh distributed, then $\chi_d^2 = 1/[(\bar{\mathbf{H}}^H \bar{\mathbf{H}})^{-1}]_{kk}$ is chi-square distributed with $2(N - K + 1)$ degrees of freedom [48]. As we have equal transmit power and equal SIQNR for all users, we drop the index k and denote the SIQNR of each stream as $\gamma_q = \gamma_0 \chi_d^2$. Based on (19) and using (12), we can express γ_0 as

$$\gamma_0 = \frac{p_u^2 \tau}{L(\alpha, p_u) [L(\alpha, p_u) + (K + \tau) p_u]} \quad (20)$$

Similarly, γ_0 for full-precision systems is obtained by substituting \mathbf{y} , $\hat{\mathbf{H}}$, and \mathbf{e} into (16) and (17). It follows that

$$\gamma_0 = \frac{p_u \sigma_h^2}{K p_u \sigma_e^2 + 1} = \frac{p_u^2 \tau}{1 + (K + \tau) p_u} \quad (21)$$

where σ_h^2 and σ_e are described in (8).

Using the previous results in [38] (for perfect CSI) together with our current findings in (20) and (21), we summarize the values of γ_0 in Table II for different scenarios, based on the assumed channel information (\mathbf{H} or its estimate $\hat{\mathbf{H}}_q$) and quantization quality (full precision or coarse quantization). We evaluate the consistency of expressions in Table II and observe the following properties.

TABLE II: Values of γ_0 for different scenarios at uplink.

| | Full precision | low resolution |
|---------------|---|---|
| Perfect CSI | p_u | $\frac{p_u}{L(\alpha, p_u)}$ |
| Imperfect CSI | $\frac{p_u^2 \tau}{1 + (K + \tau) p_u}$ | $\frac{p_u^2 \tau}{L(\alpha, p_u) [L(\alpha, p_u) + (K + \tau) p_u]}$ |

A. Increasing the Quantization Resolution

As we increase the bit-resolution b for ADCs, the value of α approaches 1, and $L(\alpha, p_u) \rightarrow 1$. Thus, both expressions of γ_0 at the right hand column, for low-resolution quantization with either full channel knowledge \mathbf{H} or an estimate $\hat{\mathbf{H}}_q$, converge to their corresponding full-precision formulas.

B. Increasing the Transmit Power

When the transmit power p_u (and the SNR per user) goes to infinity, the value of γ_0 in both expressions for full-precision quantized system (with \mathbf{H} or $\hat{\mathbf{H}}$) goes to infinity and therefore the BER approaches zero. On the other side, considering low resolution quantization, for perfect CSI we have

$$\gamma_0 \xrightarrow{p_u \rightarrow \infty} \frac{\alpha}{K(1 - \alpha)} \quad (22)$$

whereas for imperfect CSI (using $\hat{\mathbf{H}}_q$), it is

$$\gamma_0 \xrightarrow{p_u \rightarrow \infty} \frac{\alpha}{K(1 - \alpha)} \frac{\alpha \tau}{(K + \alpha \tau)} \quad (23)$$

If we assume a pilot length $\tau = K$, then the limit of γ_0 in (23) equals $\frac{\alpha}{K(1 - \alpha)} \frac{\alpha}{(1 + \alpha)}$. Table I indicates that $\frac{\alpha}{1 + \alpha} \rightarrow \frac{1}{2}$ as $\alpha \rightarrow 1$ with increasing bit resolution. As a result, we see that even with $p_u \rightarrow \infty$, the SINR of the case with imperfect CSI (channel estimate $\hat{\mathbf{H}}_q$) is about half of its value for perfect CSI. Therefore, we need to increase the pilot length as well, to compensate the effects of low-resolution quantization.

C. Increasing the Pilot Length

Increasing the pilot length τ toward infinity, both expressions of γ_0 for imperfect CSI ($\hat{\mathbf{H}}$ or $\hat{\mathbf{H}}_q$) in the last row of Table II, would be equal to their corresponding expressions with full CSI in the row above. The reason for such behavior is that the estimation error (σ_e^2 or $\sigma_{e_q}^2$) for both cases of having $\hat{\mathbf{H}}$ or $\hat{\mathbf{H}}_q$ goes to zero when $\tau \rightarrow \infty$. However, as shown in (14), a larger pilot length τ_q is required for a low-resolution quantized system, to achieve the same performance as the full-precision quantized system with the pilot length τ . As we have seen from previous discussions, the SINR loss of the coarsely-quantized system can be compensated by increasing either the pilot length or the transmit power of the users. Now we will explore this issue in more detail.

We denote the pair of the transmit power and the pilot length for the full-precision and low-resolution quantized systems by (p_u, τ) and (p_{uq}, τ_q) , respectively. Returning to Table II, to achieve the same γ_0 for both coarse quantization and full precision, we have

$$\tau_q \geq \frac{p_u^2 \tau L(\alpha, p_{uq}) [L(\alpha, p_{uq}) + K p_{uq}]}{p_{uq}^2 [1 + (K + \tau) p_u] - p_{uq} p_u^2 \tau L(\alpha, p_{uq})} \quad (24)$$

$$\begin{aligned}
\mathbb{E}\{\mathbf{n}_e \mathbf{n}_e^H\} &= (\hat{\mathbf{H}}_q^H \hat{\mathbf{H}}_q)^{-1} \hat{\mathbf{H}}_q^H \left[\mathbb{E}\{p_u \mathbf{e}_q \mathbf{s} \mathbf{s}^H \mathbf{e}_q^H\} + \mathbb{E}\{\mathbf{n} \mathbf{n}^H\} + \frac{1}{\alpha^2} \mathbb{E}\{\mathbf{n}_q \mathbf{n}_q^H\} \right] \hat{\mathbf{H}}_q (\hat{\mathbf{H}}_q^H \hat{\mathbf{H}}_q)^{-1} \\
&= (\hat{\mathbf{H}}_q^H \hat{\mathbf{H}}_q)^{-1} \hat{\mathbf{H}}_q^H \left[K p_u \sigma_{e_q}^2 \mathbf{I}_N + \mathbf{I}_N + \frac{(1-\alpha)}{\alpha} \text{diag}(p_u \mathbf{H} \mathbf{H}^H + \mathbf{I}_N) \right] \hat{\mathbf{H}}_q (\hat{\mathbf{H}}_q^H \hat{\mathbf{H}}_q)^{-1} \\
&= [K p_u \sigma_{e_q}^2 + 1 + \frac{(1-\alpha)}{\alpha} (K p_u + 1)] (\hat{\mathbf{H}}_q^H \hat{\mathbf{H}}_q)^{-1} = [K p_u \sigma_{e_q}^2 + L(\alpha, p_u)] (\hat{\mathbf{H}}_q^H \hat{\mathbf{H}}_q)^{-1} \quad (17)
\end{aligned}$$

Any pair of transmit power and pilot length values (p_{uq}, τ_q) that satisfies (24), can guarantee an equal or larger SINR for the coarsely quantized system in comparison to the full-precision quantized system with power/pilot settings (p_u, τ) . However, the denominator of inequality in (24) may be negative for some cases which means we have no solution for (p_{uq}, τ_q) to compensate the SINR loss of low-resolution quantization.

To evaluate the BER performance of the quantized MIMO system, we start from the BER of uncoded M-ary QAM modulation over an AWGN channel in a single-input single-output (SISO) system, which is given by [49]:

$$P_b(\gamma) = \sum_{k=1}^{\log_2 \sqrt{M}} \sum_{i=0}^{(1-2^{-k})\sqrt{M}-1} F(k, i) Q\left(\sqrt{\frac{3(2i+1)^2 \gamma}{M-1}}\right) \quad (25)$$

where γ is the SNR for the AWGN channel, and the coefficient $F(k, i)$ is defined as:

$$F(k, i) = \frac{2(-1)^{\lfloor \frac{i \cdot 2^{k-1}}{\sqrt{M}} \rfloor} \left(2^{k-1} - \lfloor \frac{i \cdot 2^{k-1}}{\sqrt{M}} + \frac{1}{2} \rfloor\right)}{\sqrt{M} \log_2 \sqrt{M}} \quad (26)$$

where $\lfloor \cdot \rfloor$ is the integer operator. Then, BER of a quantized MIMO system can be derived from (25) by replacing γ with γ_q . Since $\gamma_q = \gamma_0 \chi_d^2$ is a function of the random variable χ_d^2 , the average BER over a Rayleigh fading channel is calculated by taking the expectation of P_b over χ_d^2 as follows:

$$\text{BER} = \mathbb{E}_{\chi_d^2} \{P_b(\gamma_0 x)\} = \int P_b(\gamma_0 x) f_{\chi_d^2}(x) dx \quad (27)$$

where $f_{\chi_d^2}(x)$ is the probability density function of χ_d^2 with $d = 2(N - K + 1)$ degrees of freedom. By substituting (25) into (27) and solving it (see Appendix D), a tight BER approximation of the quantized MIMO system, which accounts for the effects of low-resolution quantization and channel estimation error, can be obtained as follows:

$$\text{BER} = \sum_{k=1}^{\log_2 \sqrt{M}} \sum_{i=0}^{(1-2^{-k})\sqrt{M}-1} F(k, i) B(\mu_i) \quad (28)$$

where $B(\mu_i)$ is:

$$B(\mu_i) = \left(\frac{1-\mu_i}{2}\right)^{N-K+1} \sum_{j=0}^{N-K} \binom{N-K+j}{j} \left(\frac{1+\mu_i}{2}\right)^j \quad (29)$$

and using γ_0 from (20) for the quantized system under imperfect CSI, the expression for μ_i can be rewritten as

$$\mu_i = \sqrt{\frac{3(2i+1)^2 p_u^2 \tau}{2(M-1)L(\alpha, p_u)[L(\alpha, p_u) + (K+\tau)p_u] + 3(2i+1)^2 p_u^2 \tau}} \quad (30)$$

Since the $B(\mu_i)$ values are rapidly decreasing for $i > 1$, we can further simplify (28) by keeping only two dominant terms at $i = 0, 1$:

$$\text{BER} \cong \frac{2(\sqrt{M}-1)}{\sqrt{M} \log_2 \sqrt{M}} B(\mu_0) + \frac{2(\sqrt{M}-2)}{\sqrt{M} \log_2 \sqrt{M}} B(\mu_1) \quad (31)$$

We explore the accuracy of such an approximation for BER performance in the following section by performing numerical analysis.

V. SIMULATION RESULTS

In this section, we validate the proposed analytical expressions for the channel estimation error and BER, as derived in (12) and (31), using Monte Carlo simulations. Their accuracy is assessed considering different quantization resolutions, modulation orders, and system configurations. The results also show how the analytical framework enables the design of compensation strategies to mitigate the impact of coarse quantization.

Additionally, we evaluate several practical scenarios to demonstrate how our proposed expressions can guide the selection of system parameters in low-resolution massive MIMO deployments. These results show that performance levels comparable to full-precision systems can be achieved while meeting power and BER constraints.

For each channel realization, a long sequence (10^5 to 10^6 symbols) of equi-probable M-QAM symbols is generated per user. The received vector \mathbf{y} is computed using (1) and quantized at each antenna using the non-linear quantizers described in [38], [50].

A. Channel Estimation

Equation (14) demonstrates that, by properly tuning p_{uq} and τ_q , the channel estimation error in a low-resolution quantized system can be made virtually indistinguishable from that of its unquantized equivalent.

Table III illustrates this by showing the required values of τ_q for $p_{uq} = 0$ and 3 dB, and for $K = 10$ and 20 users, assuming τ and $p_u = 0$ dB for the unquantized case. For instance, with $K = 20$, $p_u = 0$ dB, and 3-bit resolution ADCs ($b = 3$), the condition $\tau_q \geq 1.75\tau$ must be satisfied. This implies that the pilot sequence length in a 3-bit quantized system needs to be approximately 1.75 times longer to match the performance of the full-precision system. However, by increasing the transmit power by 3 dB, the requirement is relaxed to $\tau_q \geq 1.23\tau$. Figure 2 presents the behavior of the channel estimation error variance $\sigma_{e_q}^2$ as a function of the transmit power p_{uq} in (a) and

TABLE III: Required values of τ_q from (14) for a quantized system using b -bit ADCs, to match the channel estimation error of the unquantized case with a given τ pilots, $K = 10, 20$ users and $p_u = 0$ dB.

| | b | 1 | 2 | 3 | 4 |
|-------------------------|---------------|-------------|------------|------------|------------|
| $K = 10, p_{uq} = 0$ dB | $\tau_q \geq$ | 7.28τ | 2.46τ | 1.39τ | 1.11τ |
| $K = 10, p_{uq} = 3$ dB | $\tau_q \geq$ | 6.49τ | 1.90τ | 0.88τ | 0.60τ |
| $K = 20, p_{uq} = 0$ dB | $\tau_q \geq$ | 12.99τ | 3.80τ | 1.75τ | 1.20τ |
| $K = 20, p_{uq} = 3$ dB | $\tau_q \geq$ | 12.20τ | 3.23τ | 1.23τ | 0.70τ |

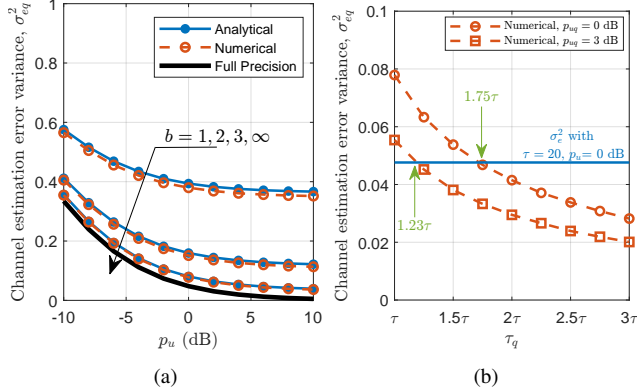


Fig. 2: Channel estimation error variance σ_{eq}^2 versus (a) p_u given $\tau = \tau_q = K$, and (b) τ_q given $K = 20$ and $b = 3$

the pilot length τ_q in (b). The analytical expressions in (12) closely align with Monte Carlo simulations assuming $K = 20$.

As a result of the above discussions, *adjusting both the transmit power and the pilot length can mitigate the performance loss in channel estimation for low-resolution quantized systems.*

B. BER Performance

We numerically validate the BER approximation in (31) for uplink M-QAM massive MIMO systems with imperfect CSI due to channel estimation errors and low-resolution quantization. This validation is performed through Monte Carlo simulations for 16-QAM, 64-QAM, and 256-QAM modulation schemes. Several practical scenarios are also presented to demonstrate the applicability of the analytical results.

We assume equal transmit power p_u for both pilot and data sequences for all users. *Note that p_u represents the SNR per user, while E_b/N_0 denotes the SNR per user per bit.* The relation between p_u and E_b/N_0 is given by:

$$p_u = \frac{\sigma_s^2}{\sigma_n^2} = \frac{E_s}{N_0/2} = \frac{E_b \log_2 M}{N_0/2} \quad (32)$$

where σ_s^2 is the signal (or symbol) power, $\sigma_n^2 = N_0/2$ is the noise power, and N_0 is the noise power spectral density. E_s and E_b are symbol and bit energies, respectively, with $E_s = E_b \log_2 M$ for M-QAM modulations [51], and M is the modulation order. From this point onward, we use E_b/N_0 instead of p_{uq} and p_u , as defined in (32), to facilitate performance comparison across different M-QAM modulation schemes.

Figures 3 and 4 illustrate the achievable BER performance of uplink massive MIMO systems with low-resolution ADCs

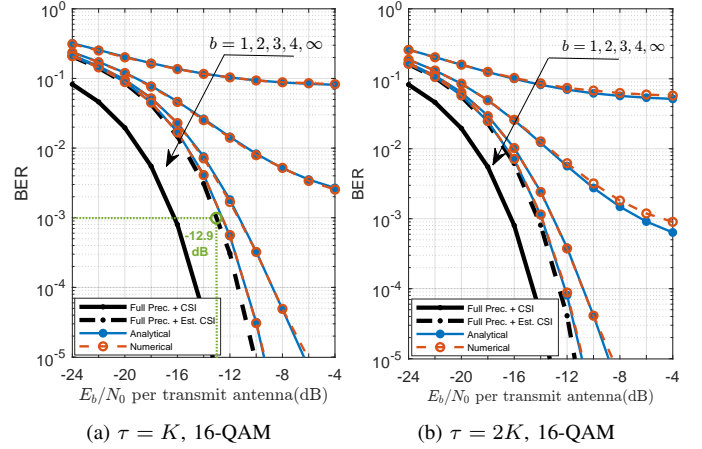


Fig. 3: BER of uplink massive MIMO with $N = 256$, $K = 20$, 16-QAM, b -bit ADCs, imperfect CSI: (a) $\tau = K$, (b) $\tau = 2K$.

and imperfect CSI (due to channel estimation error), as a function of E_b/N_0 . Both figures assume $N = 256$ antennas for BS and $K = 20$ users. In Figure 3, uncoded 16-QAM is considered with two different pilot lengths: (a) $\tau = K$ and (b) $\tau = 2K$. In contrast, Figure 4 explores higher-order modulations with fixed pilot length $\tau = K$, showing BER performance for (a) 64-QAM and (b) 256-QAM. Numerical results for all modulation schemes and bit resolutions b closely match the analytical results, confirming the validity of the BER approximation given in (31). For comparison, two BER bounds are plotted: (i) an ideal scenario with no quantization or channel estimation error (solid black line, "Full Prec. + CSI", i.e., full precision and perfect channel state information), and (ii) with channel estimation error for a given pilot length τ , but no quantization error (dashed black line, "Full Prec. + Est. Channel"). In Figure 3(a) and (b), we see that the gap between these two curves decreases as τ increases from K to $2K$, illustrating the effect of jointly varying τ and E_b/N_0 on the BER performance.

We observe a severe BER degradation when using low-resolution ADCs: 1-bit for 16-QAM, up to 2-bit for 64-QAM, and up to 3-bit for 256-QAM. Under these conditions, achieving a BER of 10^{-2} is not possible¹. Interestingly, 2-bit 16-QAM, 3-bit 64-QAM, and 4-bit 256-QAM show a similar behavior. For squared M-QAM modulations with $M = 2^{2m}$ (e.g. 4 ($m = 1$), 16 ($m = 2$), 64 ($m = 3$)), achieving reliable performance requires at least $b = m$ quantization bits.

Observation 1. *The minimum quantization bit resolution required for squared M-QAM modulations is proportional to $\log_2 \sqrt{M}$, where M is the modulation order.*

Figures 3-4 also indicate that, under constant transmit power, both longer pilots and higher quantization resolution improve BER, with quantization having a greater impact since it affects both channel estimation and data detection, whereas pilot length only influences estimation.

¹This limitation could potentially be mitigated using techniques such as spatial-domain oversampling or time-domain signal repetition. However, these are beyond the scope of this work, which focuses on uncoded M-QAM modulations.

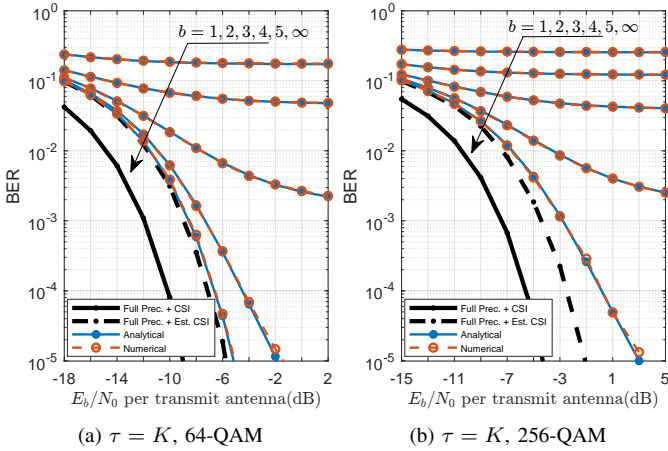


Fig. 4: BER of uplink massive MIMO with $\tau = K = 20$, b -bit ADCs, and imperfect CSI for (a) 64-QAM, (b) 256-QAM.

C. Performance in Different Scenarios

In what follows, we explore several practical scenarios to demonstrate the applicability of our proposed expressions in the context of system parameter selection.

Scenario 1: Balancing Parameters in Quantized Systems to Achieve Unquantized BER Levels

We target a BER of 10^{-3} (chosen only for simulation; other values can also be used). As shown in Figure 3a, for full-precision quantization with imperfect CSI, the required E_b/N_0 for 16-QAM is -12.9 dB. Using (24) and the target BER of 10^{-3} , Figure 5a illustrates the pilot length τ_q and E_b/N_0 required for systems with low-resolution quantizers. Each point on the curves represents a feasible $(\tau_q, E_b/N_0)$ pair that achieves the target BER, indicating either the minimum pilot length for a given E_b/N_0 or the minimum E_b/N_0 for a given τ_q .

For example, Figure 3a shows that with 2-bit 16-QAM, the target BER cannot be achieved when $\tau_q = K$. Hence, both the pilot length and transmit power must be increased. As illustrated in Figure 5a, achieving the target BER requires an E_b/N_0 of -2.8 dB with a τ_q of $1.5K$ (30 symbols) for 2-bit quantization, and -13.4 dB with a τ_q of $2.5K$ (50 symbols) for 3-bit quantization.

Figure 5b validates these findings by comparing Monte Carlo simulations and analytical results for 2-bit, 3-bit, and full-precision quantization with channel estimation (denoted as "Full Prec. + Est. CSI"). In this case, without quantization error, the target BER is achieved using $\tau = K$ and an E_b/N_0 of -12.9 dB. In contrast, 2-bit quantization with $\tau_q = 1.5K$ requires an E_b/N_0 of -2.8 dB and an additional 10.6 dB of power, which is impractical. However, 3-bit quantization with a τ_q of 50 symbols ($2.5K$) achieves the target BER at a E_b/N_0 of -13.4 dB, 0.5 dB lower than the full-precision case. Other $(\tau_q, E_b/N_0)$ combinations are also possible; these are just two examples. Therefore, using (24), we can select appropriate $(\tau_q, E_b/N_0)$ pairs to compensate for coarse quantization and match the performance of full-precision systems.

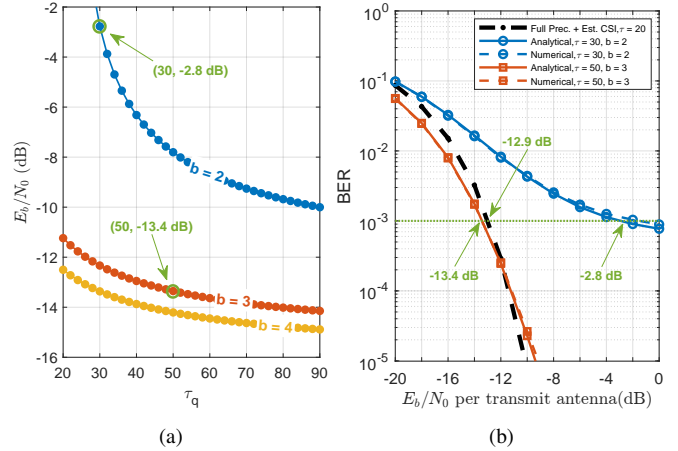


Fig. 5: (a) Required τ_q and E_b/N_0 values to achieve a BER of 10^{-3} using (24) for b -bit ADCs, $N = 256$, $K = 20$, 16-QAM. (b) BER variation with τ_q and E_b/N_0 for the same system.

Observation 2. BER performance loss of an uplink massive MIMO system due to coarse quantization can be compensated by jointly optimizing the pilot length and the transmit power.

In applications prioritizing battery life over data rate (e.g., IoT sensors), longer pilot lengths can be used to reduce transmit power while maintaining a desired BER. Conversely, high-data-rate applications (e.g., video streaming) can achieve their performance with shorter pilot lengths and adjusted transmit power.

Scenario 2: Compensating for BER Degradation as User Count Scales Up

Consider a 3-bit quantized system employing 16-QAM modulation, a pilot length of $\tau = 40$, serving $K = 20$ users with a target BER of 10^{-4} . As shown in Figure 6a, when the number of users K increases from 20 to 40, the error ratio exceeds 10^{-3} . If one attempts to compensate for this degradation solely by increasing the transmit power, Figure 6a shows that the required E_b/N_0 must rise from -10.8 dB to -0.4 dB, which is not a practical solution. The objective is to determine how parameters such as resolution, pilot length, and transmit power should be adjusted to maintain the desired quality of service.

Using (24) and the target BER of 10^{-4} , Figure 6b presents the required combinations of pilot length τ_q and E_b/N_0 for systems with 3- and 4-bit quantization, assuming $K = 40$ users. Each point on the curves represents a feasible $(\tau_q, E_b/N_0)$ pair that satisfies the target BER. For example, with $b = 3$, increasing the pilot length from 40 to 60 symbols and setting E_b/N_0 to -5.5 dB achieves the desired performance. Alternatively, for $b = 4$, the same pilot length of 40 symbols and an E_b/N_0 of -9.75 dB is sufficient to maintain the error ratio. However, this BER target cannot be met with 2-bit resolution, regardless of pilot length or transmit power, unless a lower-order modulation scheme such as QPSK is employed. Figure 6c provides Monte Carlo simulation results that validate the analytical predictions.

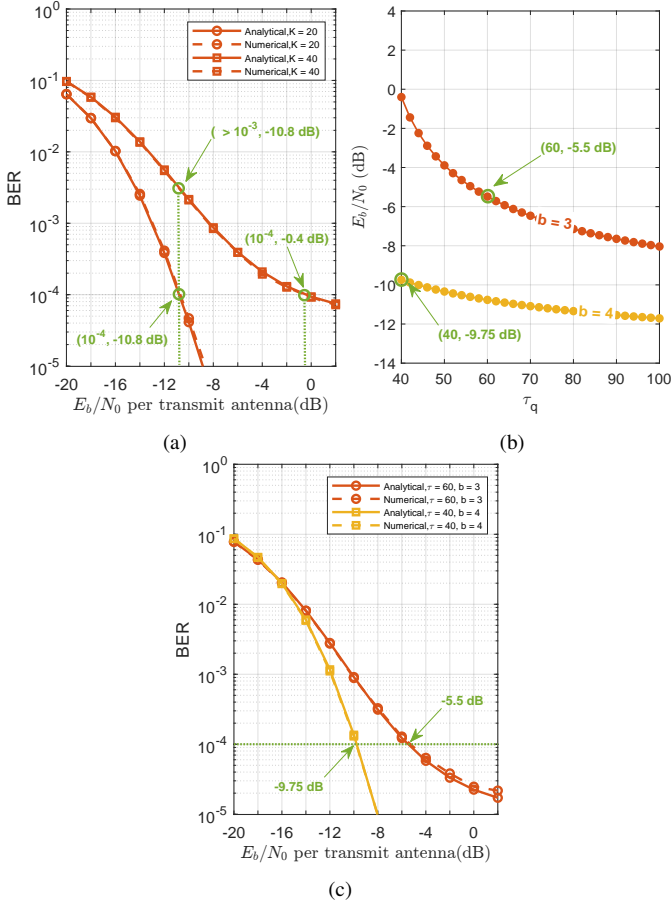


Fig. 6: BER analysis with $N = 256$ and 16-QAM modulation: (a) BER vs. E_b/N_0 with 3-bit ADCs, $K = 20, 40$ and $\tau = 40$; (b) Required $(\tau_q, E_b/N_0)$ pairs for $\text{BER} = 10^{-4}$, $K = 40$; (c) BER vs. E_b/N_0 with 3-4 bit ADCs, $K = 40$, $\tau = 40, 60$.

Scenario 3: Power-efficient ADC resolution at target BER

Although low-resolution ADCs consume less power, they degrade BER performance due to increased quantization noise. To meet a given quality-of-service (QoS) requirement, higher transmit power or a larger number of antennas is needed. In contrast, high-resolution ADCs consume more power but can achieve the same QoS with lower transmit power or fewer antennas. The goal is to find the *optimal ADC resolution and number of BS antennas* that minimize total power consumption, including both transmit and ADC processing power, while meeting a QoS constraint (e.g., $\text{BER} = 10^{-3}$). To this end, the set of (p_u, N) pairs that satisfy the target BER for each ADC resolution is derived using equation (31). For example, Figure 7a shows these pairs for $K = 20$ users, pilot length $\tau = 40$, and QPSK modulation. Then, the total power consumption is given by

$$P_{\text{total}} = K \cdot p_u + N \cdot (2P_{\text{ADC}} + P_{\text{RF}}) + P_{\text{Other}}, \quad (33)$$

where P_{RF} is the RF front-end power per antenna, P_{Other} is the power of other system components, and P_{ADC} is the ADC power consumption at the BS, given by [52]:

$$P_{\text{ADC}} = \text{FOM} \cdot f_s \cdot 2^b, \quad (34)$$

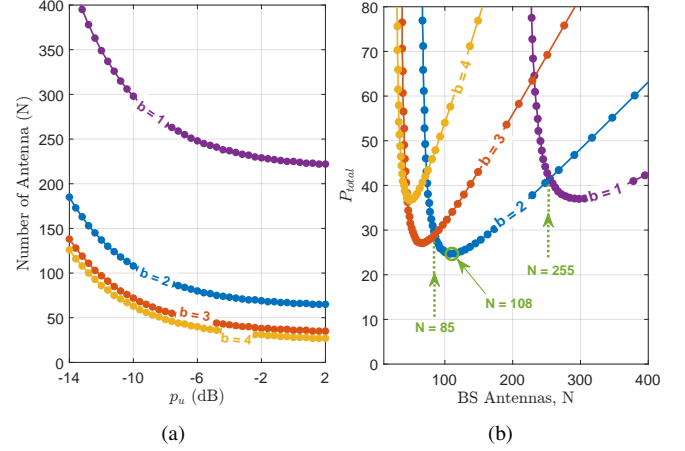


Fig. 7: (a) Required (N, p_u) pairs to achieve $\text{BER} = 10^{-3}$ for QPSK, $K = 20$, and $\tau = 40$, under 1–4 bit quantization. (b) Corresponding total power consumption P_{total} versus N using values from (a).

with the figure of merit (FOM), defined as the energy consumed per conversion step (in fJ/conversion step), and f_s representing the sampling frequency. The values of P_{RF} and P_{Other} are assumed to be constant. For simulation purposes, we use $\text{FOM} = 1432.1$ fJ/conversion step and $f_s = 100$ MHz.

Figure 7b plots the total power consumption P_{total} versus the number of antennas N for 1- to 4-bit quantization levels. For each resolution b , the corresponding (p_u, N) pair that satisfies the BER constraint is obtained from Figure 7a and used to compute P_{total} . As observed, the minimum total power occurs at $b = 2$ bits and $N = 108$ antennas.

Another insight from Figure 7b is the crossing point between the P_{total} curves for 1-bit and 2-bit quantization at $N = 255$. For antenna counts below this threshold (with a target BER of 10^{-3} and $\tau = 40$), a system with 1-bit ADCs consumes more power. This is because the higher transmit power required to meet the BER target with 1-bit resolution outweighs the power savings from using lower-resolution ADCs. Similarly, a crossing point at $N = 85$ indicates that for systems with a small number of BS antennas, 3- and 4-bit quantization are more energy-efficient than 1- and 2-bit configurations.

Scenario 4: Minimum Antennas Needed to Support a Given Number of Users at a Desired BER

In this scenario, we investigate the minimum number of BS antennas (N_{min}) required to support a given number of users K at a target BER of 10^{-3} . Assuming 16-QAM modulation, a transmit power of -8 dB in terms of E_b/N_0 , and a pilot length of $\tau = 30$, the N_{min} values for various quantization resolutions are derived using (31) and illustrated in Figure 8a. For instance, when $K = 20$, the required number of antennas for 2-, 3-, and 4-bit resolutions are 308, 141, and 98, respectively. Figure 8b presents the BER curves from both analytical analysis and Monte Carlo simulations, confirming that at $E_b/N_0 = -8$ dB, the target BER is reliably achieved for the corresponding N_{min} at each resolution level.

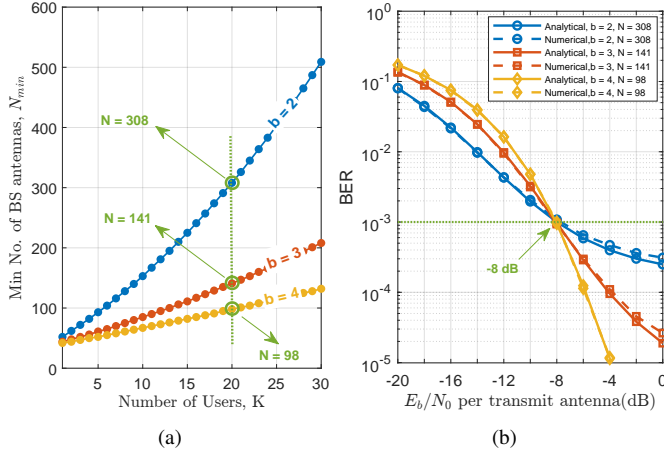


Fig. 8: (a) Min. number of BS antennas N_{\min} required to achieve a BER of 10^{-3} vs. number of users K for 2–4 bit ADCs, assuming 16-QAM and $\tau=30$. (b) BER vs. E_b/N_0 for $K=20$ using the N_{\min} values from (a).

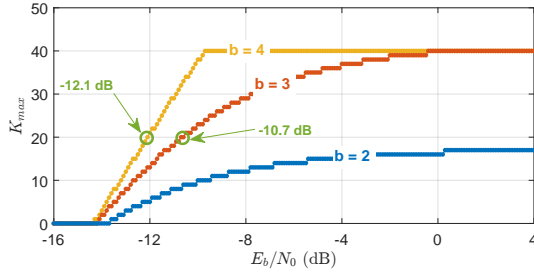


Fig. 9: Max. number of supportable users K_{\max} vs. E_b/N_0 for 2–4 bit quantization, with 16-QAM, $N=256$, $\tau=40$, and a target BER of 10^{-4} .

Scenario 5: Max. Number of users supportable at target BER

This scenario aims to determine the maximum number of supported users (K_{\max}) for each resolution, ensuring that the system's BER remains within the acceptable range (i.e., $\text{BER} \leq 10^{-4}$). We assume a configuration with $N = 256$ antennas, a pilot length of $\tau = 40$, and 16-QAM modulation. By using equation (31), Figure 9 presents the derived K_{\max} values for different resolutions under varying transmit power levels. For example, with this antenna setup, up to 20 users can be supported at 3-bit and 4-bit resolutions, corresponding to E_b/N_0 values of -10.7 dB and -12.1 dB, respectively. However, at 2-bit resolution, supporting 20 users with a $\text{BER} \leq 10^{-4}$ is not feasible at any transmit power. These findings are consistent with the Monte Carlo simulation results shown in Figure 3b.

VI. CONCLUSION

In this work, we analyzed the impact of low-resolution quantization on channel estimation and BER performance for uplink massive MIMO systems under imperfect CSI. Closed-form expressions were derived for the LMMSE channel estimator, SIQNR, and a tight BER approximation for uncoded M-QAM with zero-forcing detection. Results show that quantization-induced degradation can be effectively mitigated by jointly optimizing pilot length and transmit power for any ADC resolution.

Evaluations across five practical scenarios confirm the applicability of the proposed framework. We showed how it can be applied to balance parameters to match unquantized BER, compensate for increasing user counts, and select power-efficient ADC resolutions. For QPSK at a BER of 10^{-3} , 2-bit ADCs minimize total power consumption in moderate antenna configurations, while 1-bit quantization becomes more efficient as the array size grows.

Overall, the framework enables accurate and computationally efficient performance prediction, offering a practical alternative to computationally intensive Monte Carlo simulations, and guides the design of energy- and cost-efficient massive MIMO systems with low-resolution ADCs.

APPENDIX A QUANTIZED CHANNEL ESTIMATE

In order to prove (10), we need to substitute the quantized received signal vector \mathbf{Y}_{pq} from (9) for \mathbf{Y}_p in (6) and solve it again as follows:

$$\begin{aligned} \hat{\mathbf{H}}_q &= \arg \min_{\mathbf{W}} \mathbb{E} \left\{ \left\| \mathbf{H} - (\alpha\sqrt{p_u} \mathbf{H} \mathbf{S}_p + \mathbf{N}_e) \mathbf{W} \right\|_F^2 \right\} \\ &= \arg \min_{\mathbf{W}} \mathbb{E} \left\{ \text{Tr} \left[(\mathbf{H} - \alpha\sqrt{p_u} \mathbf{H} \mathbf{S}_p \mathbf{W} - \mathbf{N}_e \mathbf{W})^H \right. \right. \\ &\quad \left. \left. \times (\mathbf{H} - \alpha\sqrt{p_u} \mathbf{H} \mathbf{S}_p \mathbf{W} - \mathbf{N}_e \mathbf{W}) \right] \right\} \\ &= \arg \min_{\mathbf{W}} \text{Tr} \left[\mathbb{E} \left\{ (\mathbf{H} - \alpha\sqrt{p_u} \mathbf{H} \mathbf{S}_p \mathbf{W} - \mathbf{N}_e \mathbf{W})^H \right. \right. \\ &\quad \left. \left. \times (\mathbf{H} - \alpha\sqrt{p_u} \mathbf{H} \mathbf{S}_p \mathbf{W} - \mathbf{N}_e \mathbf{W}) \right\} \right] \quad (35) \end{aligned}$$

with the assumption of uncorrelated \mathbf{H} and \mathbf{N}_e , and having $\mathbb{E}\{\mathbf{H}^H \mathbf{H}\} = N \mathbf{I}_K$ and $\mathbb{E}\{\mathbf{N}_e^H \mathbf{N}_e\} = N \sigma_{N_e}^2 \mathbf{I}_K$, we have

$$\begin{aligned} \hat{\mathbf{H}}_q &= \arg \min_{\mathbf{W}} \text{Tr} \left[N \mathbf{I}_K - \alpha\sqrt{p_u} N \mathbf{S}_p^H \mathbf{W} - \alpha\sqrt{p_u} N \mathbf{W}^H \mathbf{S}_p^H \right. \\ &\quad \left. + \alpha^2 p_u N \mathbf{W}^H \mathbf{S}_p^H \mathbf{S}_p \mathbf{W} + N \sigma_{N_e}^2 \mathbf{W}^H \mathbf{W} \right] \quad (36) \end{aligned}$$

Assuming

$$\begin{aligned} \mathbf{C} &= \text{Tr} \left[N \mathbf{I}_K - \alpha\sqrt{p_u} N \mathbf{S}_p^H \mathbf{W} - \alpha\sqrt{p_u} N \mathbf{W}^H \mathbf{S}_p^H \right. \\ &\quad \left. + \alpha^2 p_u N \mathbf{W}^H \mathbf{S}_p^H \mathbf{S}_p \mathbf{W} + N \sigma_{N_e}^2 \mathbf{W}^H \mathbf{W} \right], \end{aligned}$$

the optimal \mathbf{W} can be found from the points where the first derivatives of \mathbf{C} (with respect to \mathbf{W}) equal to zero, as below

$$\begin{aligned} \frac{\partial \mathbf{C}}{\partial \mathbf{W}} &= -\alpha\sqrt{p_u} N \mathbf{S}_p^T + \alpha^2 p_u N (\mathbf{W}^H \mathbf{S}_p^H \mathbf{S}_p)^T \\ &\quad + N \sigma_{N_e}^2 (\mathbf{W}^H)^T = 0 \quad (37) \end{aligned}$$

Solving 37 and substituting $\sigma_{N_e}^2$ (see Appendix C), we have

$$\begin{aligned} \mathbf{W} &= \frac{1}{\alpha} \sqrt{p_u} \mathbf{S}_p^H (p_u \mathbf{S}_p \mathbf{S}_p^H + [1 + (\frac{1-\alpha}{\alpha})(K p_u + 1)] \mathbf{I}_K)^{-1} \\ &= \frac{1}{\alpha} \sqrt{p_u} \mathbf{S}_p^H (p_u \mathbf{S}_p \mathbf{S}_p^H + L(\alpha, p_u) \mathbf{I}_K)^{-1} \quad (38) \end{aligned}$$

APPENDIX B
CHANNEL ESTIMATION ERROR

To find the results in (12), we need to use $\mathbf{S}_p \mathbf{S}_p^H = \tau \mathbf{I}_K$ in (10) as follows:

$$\begin{aligned} \hat{\mathbf{H}}_q &= \frac{1}{\alpha} \sqrt{p_u} \mathbf{Y}_{qp} \mathbf{S}_p^H (\tau p_u \mathbf{I}_K + L(\alpha, p_u) \mathbf{I}_K)^{-1} \\ &= \frac{\sqrt{p_u}}{\alpha [\tau p_u + L(\alpha, p_u)]} \mathbf{Y}_{qp} \mathbf{S}_p^H \end{aligned} \quad (39)$$

substituting \mathbf{Y}_{pq} from (9) we have

$$\begin{aligned} \hat{\mathbf{H}}_q &= \frac{\sqrt{p_u}}{\alpha [\tau p_u + L(\alpha, p_u)]} (\alpha \sqrt{p_u} \mathbf{H} \mathbf{S}_p + \mathbf{N}_e) \mathbf{S}_p^H \\ &= \frac{\tau p_u}{[\tau p_u + L(\alpha, p_u)]} \mathbf{H} + \frac{\sqrt{p_u}}{\alpha [\tau p_u + L(\alpha, p_u)]} \mathbf{N}_e \mathbf{S}_p^H \end{aligned} \quad (40)$$

where the (i, j) entry of $\hat{\mathbf{H}}_q$ is given by

$$\begin{aligned} \hat{h}_{qij} &= \frac{\tau p_u}{[\tau p_u + L(\alpha, p_u)]} h_{ij} \\ &+ \frac{\sqrt{p_u}}{\alpha [\tau p_u + L(\alpha, p_u)]} \sum_{k=0}^{\tau} \mathbf{N}_e(i, k) \mathbf{S}_p^*(k, j) \end{aligned} \quad (41)$$

Variance of \hat{h}_{qij} can be calculated as below:

$$\begin{aligned} \mathbb{E}\{|\hat{h}_{qij}|^2\} &= \mathbb{E}\left\{\left|\frac{\tau p_u}{[\tau p_u + L(\alpha, p_u)]} h_{ij}\right|^2\right\} \\ &+ \mathbb{E}\left\{\left|\frac{\sqrt{p_u}}{\alpha [\tau p_u + L(\alpha, p_u)]} \sum_{k=0}^{\tau} \mathbf{N}_e(i, k) \mathbf{S}_p^*(k, j)\right|^2\right\} \\ &= \frac{(\tau p_u)^2}{[\tau p_u + L(\alpha, p_u)]^2} \mathbb{E}\{|h_{ij}|^2\} + \frac{p_u}{\alpha^2 [\tau p_u + L(\alpha, p_u)]^2} \\ &\times \sum_{k=0}^{\tau} \mathbb{E}\{|\mathbf{N}_e(i, k)|^2\} \mathbb{E}\{|\mathbf{S}_p^*(k, j)|^2\} \\ &= \frac{(\tau p_u)^2}{[\tau p_u + L(\alpha, p_u)]^2} + \frac{p_u}{\alpha^2 [\tau p_u + L(\alpha, p_u)]^2} \sum_{k=0}^{\tau} \sigma_{N_e}^2 \cdot 1 \\ &= \frac{(\tau p_u)^2}{[\tau p_u + L(\alpha, p_u)]^2} + \frac{\tau p_u \sigma_{N_e}^2}{\alpha^2 [\tau p_u + L(\alpha, p_u)]^2} \end{aligned} \quad (42)$$

substituting $\sigma_{N_e}^2$ from equation (46), we can simply obtain the results in (12).

APPENDIX C
VARIANCE OF THE NOISE MATRIX \mathbf{N}_e

The (i, j) entry of the noise matrix \mathbf{N}_e can be expressed as follows

$$n_e(i, j) = \alpha n_p(i, j) + n_{qp}(i, j) \quad (43)$$

where the variance $\sigma_{N_e}^2$ is

$$\sigma_{N_e}^2 = \mathbb{E}\{|n_e(i, j)|^2\} - |\mathbb{E}\{n_e(i, j)\}|^2 \quad (44)$$

The second term on the right hand side equals to zero. Because

$$\mathbb{E}\{n_e(i, j)\} = \alpha \mathbb{E}\{n_p(i, j)\} + \mathbb{E}\{n_{qp}(i, j)\} = 0 \quad (45)$$

The other term can be simplified as follows:

$$\begin{aligned} \mathbb{E}\{|n_e(i, j)|^2\} &= \mathbb{E}\{n_e(i, j) n_e^*(i, j)\} \\ &= \alpha^2 \mathbb{E}\{|n_p(i, j)|^2\} + \alpha \mathbb{E}\{n_p(i, j) n_{qp}^*(i, j)\} \\ &+ \alpha \mathbb{E}\{n_p^*(i, j) n_{qp}(i, j)\} + \mathbb{E}\{|n_{qp}(i, j)|^2\} \\ &= \alpha^2 + \alpha(1 - \alpha)(K p_u + 1) \end{aligned} \quad (46)$$

Note that samples of additive noise and quantization noise are uncorrelated in the above equation.

APPENDIX D
BER FOR M -QAM MODULATIONS

To obtain (28), we substitute (25) into (27), yielding:

$$\text{BER} = \sum_{k=1}^{\log_2 \sqrt{M}} \sum_{i=0}^{(1-2^{-k})\sqrt{M}-1} \left\{ F(k, i) \int_0^\infty Q\left(\sqrt{\frac{3(2i+1)^2}{M-1} \gamma_0 x}\right) f_{\chi_d^2}(x) dx \right\} \quad (47)$$

To solve the above integral, we use the following [51]

$$\int_0^\infty Q(\sqrt{cx}) f_{\chi_d^2}(x) dx = \left(\frac{1-\mu}{2}\right)^{\frac{d}{2}-1} \sum_{j=0}^{\frac{d}{2}-1} \binom{\frac{d}{2}-1+j}{j} \left(\frac{1+\mu}{2}\right)^j \quad (48)$$

where

$$\mu = \sqrt{\frac{c}{2+c}}, \quad c = \frac{3(2i+1)^2}{M-1} \gamma_0 \quad (49)$$

By substituting γ_0 from (20) into c and with some math, we obtain (28), (29) and (30).

REFERENCES

- [1] Z. Wang, J. Zhang, H. Du, D. Niyato, S. Cui, B. Ai, M. Debbah, K. B. Letaief, and H. V. Poor, "A tutorial on extremely large-scale MIMO for 6G: Fundamentals, signal processing, and applications," *IEEE Communications Surveys & Tutorials*, vol. 26, no. 3, pp. 1560–1605, 2024.
- [2] Y. Zhang, W. Xia, H. Zhao, Y. Mao, J. Zhang, and G. Zheng, "Enhancing uplink performance for cell-free massive MIMO with low-resolution ADCs by RSMA," *IEEE Journal on Selected Areas in Communications*, vol. 43, no. 3, pp. 720–735, March 2025.
- [3] H. Gao, D. Liu, C. Sun, and Z. Zhang, "Energy efficiency analysis and optimization for millimeter-wave MIMO with variable-resolution ADCs," *IEEE Transactions on Vehicular Technology*, vol. 73, no. 3, pp. 3949–3963, March 2024.
- [4] R. Zhang, W. Tan, S. Li, and M. Tang, "Channel estimation for irs-assisted mmwave massive MIMO systems in mixed-ADC architecture," *IEEE Internet of Things Journal*, vol. 11, no. 6, pp. 9969–9978, March 2024.
- [5] B. D. Antwi-Boasiako, R. K. Ahiadormey, P. Anokye, and K.-J. Lee, "On the performance of massive MIMO full-duplex relaying with low-resolution ADCs," *IEEE Communications Letters*, vol. 26, no. 6, pp. 1259–1263, June 2022.
- [6] Y. Xiang, H. Wu, and X. Cheng, "Ergodic capacity analysis of uplink mu-mimo systems with low-resolution ADCs," *IEEE Access*, vol. 11, pp. 132 833–132 842, 2023.
- [7] L. Fan, S. Jin, C.-K. Wen, and H. Zhang, "Uplink achievable rate for massive MIMO systems with low-resolution ADC," *IEEE Communications Letters*, vol. 19, no. 12, pp. 2186–2189, Dec 2015.
- [8] D. Qiao, W. Tan, Y. Zhao, C.-K. Wen, and S. Jin, "Spectral efficiency for massive MIMO zero-forcing receiver with low-resolution ADC," in *Proc. 8th Int. Conf. Wireless Communications and Signal Processing (WCSP)*, Yangzhou, China, Oct 2016, pp. 1–5.
- [9] Y. Dong and L. Qiu, "Spectral efficiency of massive MIMO systems with low-resolution ADCs and MMSE receiver," *IEEE Communications Letters*, vol. 21, no. 8, pp. 1771–1774, Aug 2017.

- [10] S. Jacobsson, G. Durisi, M. Coldrey, U. Gustavsson, and C. Studer, "One-bit massive MIMO: Channel estimation and high-order modulations," in *2015 IEEE International Conference on Communication Workshop (ICCW)*, London, UK, 2015, pp. 1304–1309.
- [11] L. Fan, D. Qiao, S. Jin, C.-K. Wen, and M. Matthaiou, "Optimal pilot length for uplink massive MIMO systems with low-resolution ADC," in *2016 IEEE Sensor Array and Multichannel Signal Processing Workshop (SAM)*, Rio de Janeiro, Brazil, 2016, pp. 1–5.
- [12] Y. Li, C. Tao, G. Seco-Granados, A. Mezghani, A. L. Swindlehurst, and L. Liu, "Channel estimation and performance analysis of one-bit massive MIMO systems," *IEEE Transactions on Signal Processing*, vol. 65, no. 15, pp. 4075–4089, Aug 2017.
- [13] S. Jacobsson, G. Durisi, M. Coldrey, U. Gustavsson, and C. Studer, "Throughput analysis of massive MIMO uplink with low-resolution ADCs," *IEEE Transactions on Wireless Communications*, vol. 16, no. 6, pp. 4038–4051, June 2017.
- [14] S. Ghacham, M. Benjillali, L. Van der Perre, and Z. Guennoun, "Rate analysis of uplink massive MIMO with low-resolution ADCs and zf detectors over rician fading channels," *IEEE Communications Letters*, vol. 23, no. 9, pp. 1631–1635, Sept 2019.
- [15] T. Liu, J. Tong, Q. Guo, J. Xi, Y. Yu, and Z. Xiao, "On the performance of massive MIMO systems with low-resolution ADCs and MRC receivers over rician fading channels," *IEEE Systems Journal*, vol. 15, no. 3, pp. 4514–4524, Sept 2021.
- [16] C. Mollén, J. Choi, E. G. Larsson, and R. W. Heath, "Uplink performance of wideband massive MIMO with one-bit ADCs," *IEEE Transactions on Wireless Communications*, vol. 16, no. 1, pp. 87–100, Jan 2017.
- [17] J. Zhang, L. Dai, Z. He, S. Jin, and X. Li, "Performance analysis of mixed-ADC massive MIMO systems over rician fading channels," *IEEE Journal on Selected Areas in Communications*, vol. 35, no. 6, pp. 1327–1338, June 2017.
- [18] H. Pirzadeh and A. L. Swindlehurst, "Spectral efficiency of mixed-ADC massive MIMO," *IEEE Transactions on Signal Processing*, vol. 66, no. 13, pp. 3599–3613, July 2018.
- [19] C. Kong, C. Zhong, S. Jin, S. Yang, H. Lin, and Z. Zhang, "Full-duplex massive MIMO relaying systems with low-resolution ADCs," *IEEE Transactions on Wireless Communications*, vol. 16, no. 8, pp. 5033–5047, Aug 2017.
- [20] S. Rahimian, Y. Jing, and M. Ardakani, "Performance analysis of massive MIMO multi-way relay networks with low-resolution ADCs," *IEEE Transactions on Wireless Communications*, vol. 19, no. 9, pp. 5794–5806, Sept 2020.
- [21] P. Dong, H. Zhang, Q. Wu, and G. Y. Li, "Spatially correlated massive MIMO relay systems with low-resolution ADCs," *IEEE Transactions on Vehicular Technology*, vol. 69, no. 6, pp. 6541–6553, June 2020.
- [22] Y. Xiong, S. Sun, N. Wei, L. Liu, and Z. Zhang, "Performance analysis of massive MIMO relay systems with variable-resolution ADCs/dacs over spatially correlated channels," *IEEE Transactions on Vehicular Technology*, vol. 70, no. 3, pp. 2619–2634, March 2021.
- [23] Q. Ding, Z. Wu, X. Gao, and X. Xu, "Achievable rate and energy efficiency analysis of multiuser relay-aided massive MIMO downlink," *IEEE Systems Journal*, vol. 16, no. 2, pp. 2776–2787, June 2022.
- [24] H. Wu, Y. Xiang, and X. Cheng, "Ergodic capacity analysis and resolution optimization for uplink mu-mimo systems with mixed ADCs," *IEEE Transactions on Green Communications and Networking*, 2024.
- [25] 3GPP TS 38.211, "NR; Physical channels and modulation (Release 18)," Tech. Rep. V18.6.0, Mar. 2025.
- [26] J. Choi, D. J. Love, D. R. Brown, and M. Boutin, "Quantized distributed reception for MIMO wireless systems using spatial multiplexing," *IEEE Transactions on Signal Processing*, vol. 63, no. 13, pp. 3537–3548, July 2015.
- [27] A. K. Saxena, I. Fijalkow, and A. L. Swindlehurst, "Analysis of one-bit quantized precoding for the multiuser massive MIMO downlink," *IEEE Transactions on Signal Processing*, vol. 65, no. 17, pp. 4624–4634, Sept 2017.
- [28] P. N. Alevizos, "Low-complexity multiuser qam detection for uplink 1-bit massive MIMO," *IEEE Communications Letters*, vol. 22, no. 8, pp. 1592–1595, Aug 2018.
- [29] K. Ma and Y. Jing, "Receiver design and ser analysis of massive MIMO uplink with mixed-resolution ADCs," in *2019 IEEE Pacific Rim Conference on Communications, Computers and Signal Processing (PACRIM)*, Victoria, BC, Canada, 2019, pp. 1–6.
- [30] C. Zhang, Y. Jing, Y. Huang, and X. You, "Massive MIMO with ternary ADCs," *IEEE Signal Processing Letters*, vol. 27, pp. 271–275, 2020.
- [31] Y. Zhang, L. Huang, and J. Song, "Mpdq-based high-order qam detection scheme for massive MIMO with low-precision quantization," in *2015 IEEE Global Conference on Signal and Information Processing (GlobalSIP)*, Orlando, FL, USA, 2015, pp. 28–32.
- [32] C. Desset and L. Van der Perre, "Validation of low-accuracy quantization in massive MIMO and constellation evm analysis," in *2015 European Conference on Networks and Communications (EuCNC)*, Paris, France, 2015, pp. 21–25.
- [33] M. Temiz, E. Alsusa, and L. Danoon, "Quantized massive MIMO networks under channel coding and CSI mismatch," in *2019 European Conference on Networks and Communications (EuCNC)*, Valencia, Spain, 2019, pp. 331–336.
- [34] S. Jacobsson, G. Durisi, M. Coldrey, T. Goldstein, and C. Studer, "Quantized precoding for massive mu-mimo," *IEEE Transactions on Communications*, vol. 65, no. 11, pp. 4670–4684, Nov 2017.
- [35] S. Jacobsson, G. Durisi, M. Coldrey, and C. Studer, "Linear precoding with low-resolution dacs for massive MU-MIMO-OFDM downlink," *IEEE Transactions on Wireless Communications*, vol. 18, no. 3, pp. 1595–1609, March 2019.
- [36] J. Guerreiro, R. Dinis, and P. Montezuma, "On the impact of strong nonlinear effects on massive MIMO svd systems with imperfect channel estimates," in *2017 IEEE 86th Vehicular Technology Conference (VTC-Fall)*, Toronto, ON, Canada, 2017, pp. 1–5.
- [37] Z. Wang, "Performance analysis of UCA-OAM systems with low-resolution ADCs," *IEEE Wireless Communications Letters*, vol. 14, no. 3, pp. 741–745, March 2025.
- [38] A. Azzizadeh, R. Mohammadkhani, S. V. Makki, and E. Björnson, "Ber performance analysis of coarsely quantized uplink massive MIMO," *Signal Processing*, vol. 161, pp. 259–267, Aug 2019.
- [39] K. A. Alnajjar, P. J. Smith, and G. K. Woodward, "Low complexity v-blast for massive MIMO with adaptive modulation and power control," in *2015 International Conference on Information and Communication Technology Research (ICTRC)*, Abu Dhabi, United Arab Emirates, 2015, pp. 1–4.
- [40] Y. Zhou, C. Zhong, S. Jin, Y. Huang, and Z. Zhang, "A low-complexity multiuser adaptive modulation scheme for massive MIMO systems," *IEEE Signal Processing Letters*, vol. 23, no. 10, pp. 1464–1468, Oct 2016.
- [41] M. Li, X. Zhao, H. Liang, and F. Hu, "Deep reinforcement learning optimal transmission policy for communication systems with energy harvesting and adaptive mqam," *IEEE Transactions on Vehicular Technology*, vol. 68, no. 6, pp. 5782–5793, June 2019.
- [42] S. Mashhadi, N. Ghiasi, S. Farahmand, and S. M. Razavizadeh, "Deep reinforcement learning based adaptive modulation with outdated CSI," *IEEE Communications Letters*, vol. 25, no. 10, pp. 3291–3295, Oct 2021.
- [43] J. Mo and R. W. Heath, "Capacity analysis of one-bit quantized MIMO systems with transmitter channel state information," *IEEE Transactions on Signal Processing*, vol. 63, no. 20, pp. 5498–5512, Oct 2015.
- [44] O. Orhan, E. Erkip, and S. Rangan, "Low power analog-to-digital conversion in millimeter wave systems: Impact of resolution and bandwidth on performance," in *2015 Information Theory and Applications Workshop (ITA)*, San Diego, CA, USA, 2015, pp. 191–198.
- [45] Y. Li, C. Tao, L. Liu, A. Mezghani, and A. L. Swindlehurst, "How much training is needed in one-bit massive MIMO systems at low snr?" in *2016 IEEE Global Communications Conference (GLOBECOM)*, IEEE, 2016, pp. 1–6.
- [46] J. R. Hampton, *Introduction to MIMO communications*. Cambridge University Press, 2013.
- [47] H. Q. Ngo, E. G. Larsson, and T. L. Marzetta, "Massive MU-MIMO downlink TDD systems with linear precoding and downlink pilots," in *Communication, Control, and Computing (Allerton)*, 2013 51st Annual Allerton Conference on. IEEE, 2013, pp. 293–298.
- [48] J. H. Winters, J. Salz, and R. D. Gitlin, "The impact of antenna diversity on the capacity of wireless communication systems," *IEEE Transactions on Communications*, vol. 42, no. 234, pp. 1740–1751, 1994.
- [49] K. Cho and D. Yoon, "On the general ber expression of one- and two-dimensional amplitude modulations," *IEEE transactions on communications*, vol. 50, no. 7, pp. 1074–1080, 2002.
- [50] J. Max, "Quantizing for minimum distortion," *IRE Transactions on Information Theory*, vol. 6, no. 1, pp. 7–12, 1960.
- [51] J. Proakis and M. Salehi, *Digital communications*, 5th ed. McGraw-Hill Education, 2007.
- [52] T. Liu, J. Tong, Q. Guo, J. Xi, Y. Yu, and Z. Xiao, "Energy efficiency of massive MIMO systems with low-resolution ADCs and successive interference cancellation," *IEEE Transactions on Wireless Communications*, vol. 18, no. 8, pp. 3987–4002, Aug 2019.